A Hybrid Agent-based Model Predictive Control Scheme for Smart Community Energy System with Uncertain DGs and Loads

Xiaodi Wang, Youbo Liu, Junbo Zhao, and Junyong Liu

Abstract—A multi-agent consensus-based market scheme is proposed for the cooperation of community and multiple microgrids (MGs) in a distributed, economic and hierarchal manner. The proposed community-based market framework with frequency regulation (FR) market is formulated as a two-level scheduling problem: the global decision-making process of community agent (CA) to participate in the FR market and the interaction and control process of local MGs to achieve collaboration in response to the global target with efficient pricing rules. Specifically, the model predictive control (MPC) is integrated with the consensus-based theory to allow MG to obtain an economic and reliable dispatch in the presence of uncertainties of distributed generators and loads. Thanks to the distributed nature of the proposed scheme, its robustness to communication issues has been strengthened and a win-win situation for all energy stakeholders can be achieved. The robustness of the proposed scheme is investigated in various conditions, including different implementation strategies, communication topologies, and the level of uncertainties.

Index Terms—Community market, model predictive control (MPC), energy management, consensus-based market scheme.

I. INTRODUCTION

THE microgrid (MG) is regarded as a key block of future smart grid because of its ability to embrace wide applications of distributed generators (DGs), including conventional DGs, renewable energy sources (RESs), energy storage systems, responsive demands, etc. [1]. Meanwhile, the increasing integration of distributed RESs with stochastic features challenges the economic operation of MGs [2].

In recent years, a smart community, which is expected to be a combination of interconnected MGs, has emerged to provide additional operation flexibility and efficiency of existing MGs [3]. The exported/imported energy of geographically adjacent MGs can be diverse and complementary [4]. Thus, developing a community energy system that allows MGs to exchange information, independently trigger actions and achieve economic collaboration is a promising way to reduce the adverse effect of uncertain factors. Also, a smart community with large flexible capacity enables this energy system to participate in frequency regulation (FR) market more efficiently [5]. However, all these benefits cannot be achieved without the effective technical architecture design of the smart community [6]. It contains three main challenges: ① the participation strategy of FR, in which the flexible energy resources of the community ought to be integrated to improve the system economic performance; ② the self-scheduling of each MG, in which an intelligent energy management system (EMS) is required to obtain an economic and reliable dispatching scheme in the presence of uncertainties of DG generation and load demands; ③ the interaction and interest-coordination mechanism, where the interests of the community and each local MG need to be considered simultaneously.

This new paradigm has triggered the interest of researchers on community energy management, which has the ability to coordinate the operation of multiple MGs. To realize this synergy, the schemes adopted to address the collaboration problem can be categorized into two cases: centralized and distributed schemes. The centralized scheme is widely adopted to obtain a satisfactory result in a energy management framework of coordinated community [7], [8]. However, it leads to security/privacy issues among MGs, vulnerability to single-point failures, high requirement of information and communication technology (ICT) deployment and large computational burden for large-scale systems [9], [10]. To deal with these challenges, the distributed architecture and its associated optimization algorithms are developed [11] - [13], which are capable to find satisfactory solutions while preserving the privacy and flexible interaction of energy stakeholders [14].

In particular, establishing a community-based market with an efficient pricing mechanism is a feasible solution to facilitate MGs working in a collaborative manner [5], [6]. Multi-class energy management of a community-based market is designed in [15], where the preferences of prosumers are considered. An auction scheme to share energy storage in a community is implemented [16]. Reference [17] takes into

X. Wang, Y. Liu , and J. Liu are with the College of Electrical Engineering, Sichuan University, Chengdu 610065, China (e-mail: 18280409667@163.com; liuyoubo@scu.edu.cn; liujy@scu.edu.cn).

J. Zhao (corresponding author) is with the Department of Electrical and Computer Engineering, Mississippi State University, Starkville 39762, USA (e-mail: junbo@ece.msstate.edu).

account the self-interests of each MG and presents a hierarchical optimization method for MG community. Additionally, market-based mechanisms that coordinate multiple energy entities in a distributed manner to reach a global consensus have been widely studied. Reference [18] develops a distributed model predictive control (MPC)-based scheduling approach for a network of interconnected MGs. In addition, the dual sub-gradient algorithm [19], [20] and a bi-level two-stage robust optimal scheduling [21] are utilized to coordinate the operation of MGs, but no corresponding pricing rules are designed. Reference [22] establishes an incentive mechanism for MGs based on Nash bargaining theory to guarantee the profit of each MG through trading among MGs, and the optimization model is decomposed and solved by using the alternating direction method of multipliers (ADMM). Bargaining game [23] can effectively realize the complex interaction process among independent agents. The energy trading among multiple MGs is formulated as an unconstrained Stackelberg game in [24], where the equilibrium can be achieved through relaxation algorithms.

In summary, existing reseach on market-based mechanisms to achieve the cooperation of diverse entities is usually carried out with several drawbacks: ① most market frameworks have not been integrated into the traditional operation scheme of electricity market, e.g., FR market with strict on-line tracking requirements [10]; ② the widely used decentralized ADMM and dual sub-gradient algorithms are updated with constant or diminishing step sizes, which do not reflect explicit market supply-demand status in the collaborative transaction process; ③ the interaction process among all entities assumes that communication issues are perfectly handled with the rich deployment of ICT devices, which is not feasible in practice.

To deal with the aforementioned challenges, this paper proposes an agent-based MPC scheme for a smart community energy system with uncertain DGs and loads. It fully integrates energy resources within the community in a cooperative manner to participate in the FR market. The global target of the community to profit from the FR market can be achieved in a distributed manner through interaction and control process of local MGs with profitable transaction prices. The agent-based MPC scheme motivates local agents to enroll in the community transaction scheme and offers a win-win framework for all market stakeholders in the community. The major contributions of this paper can be summarized as follows.

1) A hybrid market framework is designed for integrating FR market with the proposed community-based market. The concepts of this framework can be easily applied to other market schemes, i.e., ancillary service market, providing potential economic benefits for the whole community.

2) An agent-based market mechanism with efficient pricing rules is established for the coordination of distributed MGs within a smart community. Specifically, the pricing rules are derived from the interaction process among all agents, which provides explicit community market information and illustrates the preferences of individual MG in the energy transaction.

3) An MPC energy management scheme is integrated with the consensus-based theory to allow MG to obtain economic and reliable dispatch. The interaction process among all agents has been spontaneously carried out based on the existing communication infrastructure within a community. Thanks to the distributed nature of the proposed scheme, its robustness to communication issues has been strengthened and a better economic performance can be achieved.

The remainder of this paper is organized as follows. Section II formulates the problem and presents the detailed mathematical model description of the proposed scheme. Case studies are carried out in Section III. And Section IV concludes the paper.

II. PROBLEM FORMULATION AND PROPOSED SCHEME

The supply and demand fluctuation of an MG not only brings adverse influence on its economic operation but also affects its market participation modes. This calls for the development of an efficient energy management framework to guarantee the economic performance of MGs. To this end, a hybrid agent-based market scheme for coordinated energy management of a smart community including multiple MGs is proposed and shown in Fig. 1.
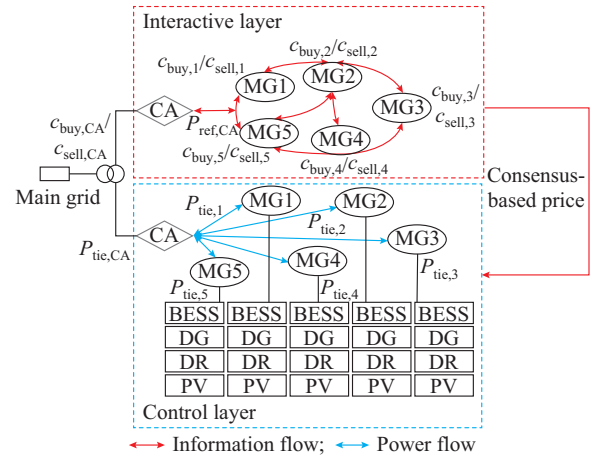

Fig. 1.   Proposed community framework.

The proposed energy management scheme is modeled as a bi-level scheduling problem: the global decision-making process of community agent (CA) to optimize FR market participation strategy of the whole community at the upper level, and the interaction and control process of local MGs at the lower level in response to the global requirements from FR market, i.e., strict energy trajectory tracking requirements over the regulation period. Specifically, the interaction among local MGs is carried out on the proposed community-based market platform, in which pricing signals are utilized to facilitate the consensus reaching process with existing communication infrastructure. It consists of the following major components.

1) CA monitors the global information based on the prediction of the community future status, and then the optimal capacity to participant in the FR market can be determined by CA. After that, the energy trajectory $P_{ref,CA}$ executed at

the lower level can be calculated once the CA received FR signal from the main grid.

2) Self-organizing MG responds to price signals and determines the control scheme of its conventional DG, battery energy storage system (BESS), demand response (DR) resources as well as the transactive energy flow with the community.

3) Local MG interacts with adjacent MGs to share information of transaction prices/quantity (i. e., $c_{\mathrm{sell},m}$, $c_{\mathrm{buy},m}$, and $P_{\mathrm{tie},m}$) iteratively so as to reach a consensus on transactive prices. Each of them iteratively updates its control scheme to optimize transactive energy flow with CA in response to price signals. Meanwhile, the energy trajectory tracking the requirement of FR program can be achieved by the coordination of MGs through iterations. Finally, from the consensus-based results, the distributed energy management of each MG can be implemented at each optimization interval in the distributed MPC framework.

In summary, the proposed scheme performs the comprehensive economic optimization within a community and MG energy management scheduling, which provides a good platform for CA to integrate MGs to participate in the FR market.

A. Upper-level Scheduling: Global Decision-making Process of CA

CA, as a higher-level autonomous entity, aims to determine optimal participation strategies in energy and FR markets operated by the main grid at the beginning of each optimization interval. Its objective function at time slot k is:

$$
\begin{aligned}
\max_{F_{\mathrm{FR}}} \sum_{h=0}^{H-1} & (c_{\mathrm{FR}}(k+h)F_{\mathrm{FR}}(k+h)- \\
& c_{\mathrm{buy,CA}}(k+h)P_{\mathrm{buy,CA}}(k+h)-c_{\mathrm{sell,CA}}(k+h)P_{\mathrm{sell,CA}}(k+h)+ \\
& \sum_{m=1}^{M}(c_{\mathrm{buy},m}(k+h)P_{\mathrm{buy},m}(k+h)-c_{\mathrm{sell},m}(k+h)P_{\mathrm{sell},m}(k+h)))
\end{aligned} \quad (1)
$$

where h is the index of prediction horizon; H is the optimization horizon; m is the index of MGs; M is the total number of MGs in the community; $c_{\mathrm{buy,CA}}$ and $c_{\mathrm{sell,CA}}$ are the buying and selling prices offered by the main grid to CA, respectively; $P_{\mathrm{buy,CA}}$ and $P_{\mathrm{sell,CA}}$ are the imported/exported power of CA from/to the main grid, respectively; $P_{\mathrm{buy},m}$ and $P_{\mathrm{sell},m}$ are the imported/exported power of MGm from/to CA, respectively; $c_{\mathrm{buy},m}$ and $c_{\mathrm{sell},m}$ are the buying and selling prices for MGm, respectively; and F_{FR} is the committed FR capacity provided for the main grid by the community. In (1), the first term represents the FR revenue, while the second term involves the transaction cost with the main grid, and the third term represents the energy transaction cost with the multiple MGs.

CA firstly initiates the bilateral trading price with MGs, i. e., buying price $c_{\mathrm{buy},m}$ and selling price $c_{\mathrm{sell},m}$, of MGm at the beginning of the scheduling interval, and predicts supply-demand status as well as the dispatchable energy capacity in the community. Then, the optimal FR capacity that CA offered to the main grid is determined accordingly. Since buying/selling prices of MGs cannot be accurately predicted and they are also changeable through interaction process at the lower level, the predicted transaction prices for all MGs are set as the initial bilateral transaction prices offered to MGs

by CA.

At real-time practice, only a fraction of committed FR capacity is requested by the main grid (averaged every 15 min), i. e., αF_{FR}. α is a scaling of the normalized regulation signal received from the main grid. Once CA receives the real regulation signal $\alpha(k)$, the optimal energy trajectory $P_{\mathrm{ref,CA}}$ of CA at time slot k can be calculated via (2).

$$
P_{\mathrm{ref,CA}}(k)=\sum_{m=1}^{M}P_{\mathrm{buy},m}(k)-\sum_{m=1}^{M}P_{\mathrm{sell},m}(k)+\alpha(k)F_{\mathrm{FR}}(k) \quad (2)
$$

Assuming that CA does not have its own flexible energy sources, the coupling energy constraints among multiple MGs should therefore be considered as follows:

$$
P_{\mathrm{tie,CA}}(k)=P_{\mathrm{buy,CA}}(k)-P_{\mathrm{sell,CA}}(k)=\sum_{m=1}^{M}(P_{\mathrm{buy},m}(k)-P_{\mathrm{sell},m}(k)) \quad (3)
$$

where $P_{\mathrm{tie,CA}}$ is the tie-line power between CA and the main grid. A positive $P_{\mathrm{tie,CA}}$ means CA needs to import the energy from the main grid and vice versa. During the operation, CA aggregates the transactive power flow of MGs to track the desired energy trajectory within the allowed tracking error bound $\varepsilon_{\mathrm{tol}}$ in a distributed manner through the scheduling process at the lower level. The constraint for tracking error can be expressed as:

$$
\left| P_{\mathrm{tie,CA}}(k)-P_{\mathrm{ref,CA}}(k)\right|\leq\varepsilon_{\mathrm{tol}} \quad (4)
$$

Note that an MG can either sell/buy energy from the main grid or the community. Thus, a MG benefits from the trading with community instead of the main grid at time slot k only if the following conditions are satisfied.

Condition 1: the selling price $c_{\mathrm{sell},m}$ offered to MGm with surplus power by the community is higher than the selling price $c_{\mathrm{sell,CA}}$ provided by the main grid.

Condition 2: the buying price $c_{\mathrm{buy},m}$ offered to MGm with deficient power by the community is lower than the buying price $c_{\mathrm{buy,CA}}$ provided by the main grid.

In order to aggregate local MGs, the transaction prices offered to MGs by the community are subject to (5).

$$
\begin{cases}
c_{\mathrm{buy}}^{\min}(k)\leq c_{\mathrm{buy},m}(k)\leq c_{\mathrm{buy,CA}}(k) \\
c_{\mathrm{sell,CA}}(k)\leq c_{\mathrm{sell},m}(k)\leq c_{\mathrm{sell}}^{\max}(k)
\end{cases} \quad (5)
$$

where $c_{\mathrm{buy}}^{\min}$ and $c_{\mathrm{sell}}^{\max}$ are the minimum buying price and the maximum selling price for MGm while MGm trades with CA, respectively.

In addition, the committed FR must be within the controllable power capacity of the whole community via (6).

$$
0\leq F_{\mathrm{FR}}(k)\leq\eta_{\mathrm{CA}}\sum_{m=1}^{M}P_{\mathrm{DG},m}^{\max}(k)+P_{\mathrm{dis},m}^{\max}(k)+\Delta P_{\mathrm{load},m}(k) \quad (6)
$$

where η_{CA} is the maximum allowable FR participation portion; $P_{\mathrm{DG},m}^{\max}$, $P_{\mathrm{dis},m}^{\max}$, and $\Delta P_{\mathrm{load},m}$ are the maximum DG output power, BESS discharging power, and load curtailment in MGm, respectively.

B. Lower-level Scheduling: MPC Control Process of Individual MG

In this subsection, the dynamic model of individual MG is presented and then the control objective functions subject to different constraints of different MG components are dis-

cussed. Each MG consists of controllable DGs, photovoltaic (PV), BESS and responsive load, and its dynamics can be formulated as:

$$E_{\text{BESS},m}(k+1)=E_{\text{BESS},m}(k)+\begin{bmatrix}0\\T\eta_{\text{ch}}\\-\dfrac{T}{\eta_{\text{dis}}}\\0\end{bmatrix}^{\text{T}}\begin{bmatrix}P_{\text{DG},m}(k)\\P_{\text{ch},m}(k)\\P_{\text{dis},m}(k)\\\Delta P_{\text{DR},m}(k)\end{bmatrix} \quad (7)$$

$$P_{\text{tie},m}(k)=\begin{bmatrix}1\\-1\\1\\1\end{bmatrix}^{\text{T}}\begin{bmatrix}P_{\text{DG},m}(k)\\P_{\text{ch},m}(k)\\P_{\text{dis},m}(k)\\\Delta P_{\text{DR},m}(k)\end{bmatrix}+\begin{bmatrix}1&-1\end{bmatrix}\begin{bmatrix}\hat{P}_{\text{PV},m}(k)\\\hat{P}_{\text{L},m}(k)\end{bmatrix} \quad (8)$$

where T is the control time interval; $P_{\text{DG},m}(k)$, $P_{\text{ch},m}(k)$, $P_{\text{dis},m}(k)$, and $\Delta P_{\text{DR},m}(k)$ are the DG output, BESS charging power, BESS discharging power, and load curtail power in MGm at time slot k, respectively; $E_{\text{BESS},m}(k)$ is the state of BESS at time slot k; $P_{\text{tie},m}(k)$ is the transaction power of MGm; $\hat{P}_{\text{PV},m}(k)$ and $\hat{P}_{\text{L},m}(k)$ are the predicted PV output and the predicted load demand, respectively; and η_{ch} and η_{dis} are BESS charging efficiency and BESS discharging efficiency, respectively.

Thus, the state space form of a MG can be formulated as follows:

$$\begin{cases}x(k+1)=Ax(k)+B_uU(k)\\y(k)=C_uU(k)+B_dW(k)\end{cases} \quad (9)$$

where A, B_u, C_u, and B_d are the coefficient matrices; $x(k)$ is the state vector that represents the state of BESS $E_{\text{BESS},m}(k)$ at time slot k; $U(k)$ is the control sequence, which consists of the dispatchable sources $P_{\text{DG},m}(k), P_{\text{ch},m}(k), P_{\text{dis},m}(k)$ and $\Delta P_{\text{DR},m}(k)$ in each MG; $y(k)$ is the system output, i. e., the transaction power $P_{\text{tie},m}(k)$ of MGm; and $W(k)$ is the vector of uncertain factors and can be expressed as $W(k)= [\hat{P}_{\text{PV},m}(k),\hat{P}_{\text{L}m}(k)]^{\text{T}}$. In practice, uncertainties are usually associated with the intermittent energy outputs of renewables $\hat{P}_{\text{PV},m}(k)$ and load demands $\hat{P}_{\text{L},m}(k)$.

The decision-making objective of an MG is to manage its dispatchable energy resources and determine the optimal transactive power to minimize the total cost while satisfying all the constraints. The local controller of a MG is designed in an MPC framework for controlling the operation process on a receding horizon. Specifically, the optimization problem of MGm at each time slot k can be expressed as:

$$\min f_m=\sum_{h=0}^{H-1}((f_{\text{DG},m}(\Delta P_{\text{DG},m}(k+h))+f_{\text{DR},m}(\Delta P_{\text{DR},m}(k+h))+$$
$$f_{\text{BESS},m}(P_{\text{ch},m}(k+h),P_{\text{dis},m}(k+h))+f_{\text{trade},m}(P_{\text{tie},m}(k+h))) \quad (10)$$

where f_m is the total costs of MGm on its optimization horizon, which covers DG operation cost $f_{\text{DG},m}$, BESS operation cost $f_{\text{BESS},m}$, DR operation cost $f_{\text{DR},m}$ and transaction cost $f_{\text{trade},m}$. At the beginning of each scheduling interval, MPC controller of MG calculates the control action sequence for time slots $[k+0,k+1,...,k+H-1]$ based on the predicted status of the MG. The first element of the computed control se-

quence will be taken as the input at time slot k. The control action for the future interval will be calculated at the beginning of the next scheduling interval. Each MG seeks the least total cost shown in (10), which is subjected to the following physical constraints.

1) Conventional DG

The fuel cost of a conventional DG can be expressed via a typical quadratic function [25] and can be written as (11).

$$f_{\text{DG},m}(P_{\text{DG},m}(k))=\alpha_{\text{DG},m}+\beta_{\text{DG},m}P_{\text{DG},m}(k)+\gamma_{\text{DG},m}P_{\text{DG},m}^2(k) \quad (11)$$

$$0\leq P_{\text{DG},m}(k)\leq P_{\text{DG},m}^{\max} \quad (12)$$

where $\alpha_{\text{DG},m}$, $\beta_{\text{DG},m}$, and $\gamma_{\text{DG},m}$ are the fuel cost coefficients of conventional DG.

2) BESS

In order to capture the charging and discharging cycles of BESS, the charging power $P_{\text{ch},m}$ and discharging power $P_{\text{dis},m}$ are separately considered and the state of BESS can be expressed as:

$$E_{\text{BESS},m}(k+1)=E_{\text{BESS},m}(k)+\eta_{\text{ch}}TP_{\text{ch},m}(k)-\frac{1}{\eta_{\text{dis}}}TP_{\text{dis},m}(k) \quad (13)$$

Generally, BESS should satisfy the constraint (14) for the safe operation and periodic utilization within the scheduling cycle.

$$\begin{cases}0\leq P_{\text{ch},m}(k)\leq P_{\text{ch},m}^{\max}\\0\leq P_{\text{dis},m}(k)\leq P_{\text{dis},m}^{\max}\\E_{\text{BESS},m}^{\min}\leq E_{\text{BESS},m}(k)\leq E_{\text{BESS},m}^{\max}\end{cases} \quad (14)$$

where $P_{\text{ch},m}^{\max}$ is the maximum charging power; and $E_{\text{BESS},m}^{\min}$ and $E_{\text{BESS},m}^{\max}$ are the lower and upper bounds of the permitted storage level, respectively.

The cost function of BESS in the scheduling period can be approximated with a quadratic function with the suitable cost coefficient $\alpha_{\text{BESS},m}$ [26] and can be written as (15).

$$f_{\text{BESS},m}(P_{\text{ch},m}(k),P_{\text{dis},m}(k))=\alpha_{\text{BESS},m}(P_{\text{ch},m}^2(k)+P_{\text{dis},m}^2(k)) \quad (15)$$

Note that simultaneously charging and discharging of BESS will lead to suboptimal solution due to the quadratic function of BESS. The theoretical proof can be found in [27].

3) Flexible Load

Based on the linear demand versus the price expression, the DR cost function of each MG can be calculated according to the quantity of power curtailment $\Delta P_{\text{DR},m}$. And the corresponding sensitiveness [24] is:

$$f_{\text{DR},m}(\Delta P_{\text{DR},m}(k))=-\frac{1}{\alpha_{\text{DR},m}}\Delta P_{\text{DR},m}^2(k)+\frac{P_{\text{L},m}(k)-\beta_{\text{DR},m}}{\alpha_{\text{DR},m}}\Delta P_{\text{DR},m}(k)$$
$$(16)$$

where $\alpha_{\text{DR},m}$ and $\beta_{\text{DR},m}$ are the sensitive parameters of flexible loads inside MGm; and $P_{\text{L},m}$ is the benchmark load of MGm.

The load of MGm can be flexibly scheduled, subjecting to the constraint (17).

$$0\leq \Delta P_{\text{DR},m}(k)\leq \eta_{\text{L},m}P_{\text{L},m}(k) \quad (17)$$

where $\eta_{\text{L},m}$ is the maximum allowable power curtailment portion.

Thus, the ultimate load of MGm can be expressed as (18).

$$P_{\text{load},m}(k) = P_{\text{L},m}(k) - \Delta P_{\text{DR},m}(k) \tag{18}$$

where $P_{\text{load},m}(k)$ is the actual load in MGm after the implementation of DR.

4) Transactive Energy Model of MG

An MG can act as a consumer to buy the power from the main grid or community when the energy output is insufficient to balance the total energy demand within the MG. Otherwise, it will act as a producer to sell power to the main grid or community. Hence, the trading cost/revenue of MG is determined by the direction of tie-line power and the associated trading price via (19).

$$f_{\text{trade}}(P_{\text{tie},m}(k)) = (c_{\text{buy},m}(k)P_{\text{buy},m}(k) - c_{\text{sell},m}(k)P_{\text{sell},m}(k))T \tag{19}$$

The trading power is limited by the power balance constraint (20) in a MG. Also, and the maximum buying power $P_{\text{buy},m}^{\max}$ and the maximum selling power $P_{\text{sell},m}^{\max}$ are determined by the transmission line capacity shown in (21).

$$P_{\text{tie},m}(k) = P_{\text{buy},m}(k) - P_{\text{sell},m}(k) = -P_{\text{PV},m}(k) - P_{\text{DG},m}(k) + P_{\text{ch},m}(k) - P_{\text{dis},m}(k) + P_{\text{load},m}(k) \tag{20}$$

$$\begin{cases} 0 \leq P_{\text{buy},m}(k) \leq P_{\text{buy},m}^{\max} \\ 0 \leq P_{\text{sell},m}(k) \leq P_{\text{sell},m}^{\max} \end{cases} \tag{21}$$

5) Uncertainties of MG

Additionally, the interval prediction method [26] is applied to estimate the lower/upper bounds of the uncertainties for an MG. The following uncertain set is provided to describe the uncertainties of PV generation and load in each MG. In this case, the actual load $P_{\text{L},m}(k)$ and PV output $P_{\text{PV},m}(k)$ in different time periods are all limited in the interval bounds that are shown as:

$$\begin{cases} P_{\text{L},m}(k) \in [\hat{P}_{\text{L},m}(k) - \Delta P_{\text{L},m}^{\max}(k), \hat{P}_{\text{L},m}(k) + \Delta P_{\text{L},m}^{\max}(k)] \\ P_{\text{PV},m}(k) \in [\hat{P}_{\text{PV},m}(k) - \Delta P_{\text{PV},m}^{\max}(k), \hat{P}_{\text{PV},m}(k) + \Delta P_{\text{PV},m}^{\max}(k)] \end{cases} \tag{22}$$

where $\Delta P_{\text{L},m}^{\max}(k)$ and $\Delta P_{\text{PV},m}^{\max}(k)$ are the maximum prediction deviations of load and PV output at time slot k, respectively.

C. Lower-level Scheduling: Interaction Process of Multiple MGs

Although each MG optimizes its scheduling scheme individually, the tracking requirement of energy trajectory from CA can only be achieved by the cooperation of all MGs. In this paper, the first-order adaptive consensus [28] algorithm is extended to achieve the developed consensus process.

Consider a community consisting of n MGs that interacts with each other based on the existing communication infrastructure. The interaction network among agents can be illustrated by a directed graph denoted as $\varsigma = \{v, \varepsilon\}$, where $v = \{1, 2, ..., M\}$ is the set of MGs and $\varepsilon \subseteq v \times v (n, m \subseteq v)$ is the edge set (interaction). In this digraph, each MG is represented by a vertex and the this digraph edge provides a communication link between MGn and its adjacent MGm. For MGm, $A_m = (n \subseteq v | (n, m) \subseteq \varepsilon)$ represents the set of its neighboring MGn. Based on these most basic elements, the row stochastic matrix $\boldsymbol{D} = (d_{nm})$ of the graph ς can be formulated as:

$$d_{nm} = \begin{cases} \dfrac{2}{z_n + z_m + \Delta} & n \in A_m \\ 1 - \displaystyle\sum_{n \in A_m} (z_n + z_m + \Delta) & n = m \\ 0 & \text{otherwise} \end{cases} \tag{23}$$

where z_m and z_n are the numbers of neighboring MGs connected with MGm and MGn, respectively; and Δ is a small positive value.

Given a strongly connected interaction topology, the adaptive consensus algorithm for the consensus-based iteration process at each iteration τ can be described as (24).

$$y_m^{\tau+1} = \sum_{n=1}^{M} d_{nm}^{\tau} y_m^{\tau} \tag{24}$$

where y_m is the output of MGm (tie-lie power flow, i.e., $P_{\text{tie},m}$), derived from the system dynamics formulation of (7); d_{nm} is a normalized distance between MGm and MGn; and τ is the τth iteration.

The power mismatch ΔP between aggregated MGs transactive energy flow and the desired energy trajectory of CA from the upper-level decision process at each time slot k are introduced into the following adaptive consensus algorithm.

$$\Delta P^{\tau}(k) = \sum_{m=1}^{M} P_{\text{tie},m}^{\tau}(k) - P_{\text{ref,CA}}(k) \tag{25}$$

Thus, the consensus-based interaction should be carefully designed to track the energy trajectory following the rule shown in (26).

$$c_m^{\tau+1}(k) = \sum_{n=1}^{M} d_{mn}^{\tau} c_m^{\tau+1}(k) + \mu \Delta P^{\tau}(k) \tag{26}$$

where μ is a positive scalar denoting the adjustment factor of power mismatch, which controls the convergence speed of the system. The increase or decrease of prices c_m^{τ} of each MG follows the sign of ΔP^{τ} at the τth iteration.

By fully considering the lower and upper limits of transaction prices, constraint (27) and constraint (28) are derived from (5). The global target at the upper level can be achieved when all MGs at the lower level reach a consensus on transaction prices. Then, the optimal community energy management scheme can be determined while satisfying various constraints.

$$c_{\text{buy},m}^{k} = \begin{cases} c_{\text{buy}}^{\min} & c_{\text{buy},m}^{\tau} \leq c_{\text{buy}}^{\min} \\ c_{\text{buy},m}^{\tau} & c_{\text{buy}}^{\min} < c_{\text{buy},m}^{\tau} < c_{\text{buy,CA}} \\ c_{\text{buy,CA}} & c_{\text{buy},m}^{\tau} \geq c_{\text{buy,CA}} \end{cases} \tag{27}$$

$$c_{\text{sell},m}^{k} = \begin{cases} c_{\text{sell}}^{\min} & c_{\text{sell},m}^{\tau} \leq c_{\text{sell}}^{\min} \\ c_{\text{sell},m}^{\tau} & c_{\text{sell}}^{\min} < c_{\text{sell},m}^{\tau} < c_{\text{sell,CA}} \\ c_{\text{sell,CA}} & c_{\text{sell},m}^{\tau} \geq c_{\text{sell,CA}} \end{cases} \tag{28}$$

where $c_{\text{buy},m}^{k}$ and $c_{\text{sell},m}^{k}$ are the ultimate consensus-based buying price and selling price of MGm, respectively.

D. Algorithm Implementation

In this subsection, a bi-level coordinated energy management algorithm is proposed to obtain the solution of the developed framework. The upper-level CA solves its own optimization problem and provides references for the local MG at the lower layer. The iterative consensus-based strategy is

then developed to exchange information with each agent, yielding global consensus solutions as the deviation from the reference energy trajectory decreases to a tolerance threshold or the maximum iteration time is reached. Detailed implementation steps at time slot k are as follows.

Step 1: MGs initiate expected trading prices $\hat{c}_{\text{buy},m}(k)$ and $\hat{c}_{\text{sell},m}(k)$ for further transactions while CA initiates the unannounced bilateral trading prices for each MG.

Step 2: the global information is monitored by CA, yielding the commitments $F_{\text{FR}}(k)$ by (1).

Step 3: once the actual value $\alpha(k)$ is provided by the main grid, $P_{\text{ref,CA}}(k)$ is calculated for the community by (2). And then, the information of $P_{\text{ref,CA}}(k)$ is shared among MGs.

Step 4: each MG updates the uncertain forecast set of $\hat{P}_{\text{L},m}(k)$ and $\hat{P}_{\text{PV},m}(k)$ for future prediction horizon at time slot k and obtains the real-time state of $P_{\text{PV},m}(k)$ and $P_{\text{L},m}(k)$. MG responds to the announced bilateral trading price signals offered by CA. As a result, an initial set of its control action U_m^0 by (10) is determined locally.

Step 5: the interaction process is implemented among local MGs and CA at iteration τ ($1 \leq \tau \leq \tau_{\max}$).

1) The interaction network $\boldsymbol{D}$ is updated among MGs.

2) The consensus-based transaction price $c_m^\tau(k)$ is updated among MGs by (25).

3) The new control sequence $U_m^\tau(k)$ of MGm at the τth iteration is updated by solving (9) based on $P_{\text{PV},m}(k)$, $P_{\text{L},m}(k)$, and $c_m^\tau(k)$.

4) The tie-line power $P_{\text{tie},m}^\tau(k)$ of each MG is updated. The energy mismatch $\Delta P^\tau(k)$ is calculated by (24).

5) If $\Delta P^\tau(k) \leq \varepsilon_{\text{tol}}$ or $\tau \geq \tau_{\max}$, the iteration will stop and the flow goes to *Step 6*; otherwise, let $\tau = \tau + 1$, and the flow goes back to 2).

Step 6: upon the completion of MG interaction, each MG applies its optimal control action $U_m^\tau(k)$ to MG.

Step 7: let $k = k + 1$ and the flow proceeds to the next cycle.

The convergence proof of the proposed method is provided in the Appendix A.

III. Simulation Results

A. Simulation Settings

Numerical simulations are conducted in a community-based scenario to evaluate the performance of the proposed method. It encompasses five MGs: MG1, MG2, MG3, MG4, and MG5. Each MG has the same basic device components, but different capacities and load profiles. The used parameters are given in the Appendix B Tables BI and BII, and the parameters shown in Table BII are drawn from [28]. The length of each time interval T is set to be 15 min, which means that the optimization problem will be solved every 15-minute interval with 3-hour prediction horizon H. The initial buying and selling prices offered by CA to all MGs are drawn from a uniform distribution with 10% heterogeneity between 60 $/MWh and 80 $/MWh. The minimum buying price and the maximum selling price for MGs are set as 40 $/MWh and 100 $/MWh, respectively. In addition, the buy-

ing and selling prices for CA to trade with the main grid are both 70 $/MWh. Historical data for FR prices and signals from PJM are extracted from [10]. According to off-line simulations, the maximum iteration time $\tau_{\max}$ of the consensus-based process is set to be 50, while the accepted tracking deviation ε_{tol} is 0.002 MW and the adjustment factor μ is 10. All simulations are carried out on a 64 bit PC with 1.99 GHz CPU and 2 GB RAM, and the YALMIP toolbox in MATLAB and CPLEX are adopted to solve the quadratic programming problem.

B. Result Analysis

1) Comparison of Different Implementations

In order to validate the effectiveness of the proposed distributed consensus-based scheme, a none-cooperating scheme and a centralized scheme [29] are used for comparison from an economic perspective. In the none-cooperating scheme, each local MG only focuses on its own local objectives and trades energy with community at the price of grid rate (i.e., both the buying price and the selling price are 70 $/MWh). For the widely used centralized scheme, CA is in charge of dispatching energy resources of all MGs to participate in FR market under the assumption that MG agents only trade with CA at the price of grid rate. All three schemes are designed in an MPC framework.

Table I reports the daily benefits and costs achieved by the proposed scheme, the centralized MPC scheme, and the none-cooperating MPC scheme. Compared with the proposed scheme, the centralized MPC scheme has provided a slightly better performance on CA cost and energy trajectory tracking, i.e., the less energy mismatch between aggregated MG energy flow and the desired energy trajectory across the day. However, the total revenue of all MGs obtained by both the centralized MPC and the none-cooperating MPC schemes are less than that by the proposed scheme. This means that the proposed scheme can bring more benefit to MGs. The reasons lie in two folds: ① in the proposed distributed scheme, the community has offered higher selling price and lower buying price for MGs compared with that of the centralized/none-cooperating schemes, which leads to CA benefit loss and MGs profit gaining; ② the centralized scheme focuses on the energy trajectory tracking instead of the local interest of each MG. Moreover, although CA may suffer certain economic loss from trading with MGs, the participation of FR market will bring CA with more revenue to cover its transaction loss. In this regard, the proposed market framework has established a win-win situation for all energy stakeholders. Additionally, it can be noticed that the total operation cost of all MGs is $1066.4 for the proposed scheme, higher than $1036.4 for the centralized one. But for large-scale interaction problems, it can be acceptable to obtain a sub-optimal settlement in exchange of more flexibility. In addition, compared with the none-cooperating scheme, Table I demonstrates that the improvement of MG benefits by the proposed scheme mainly attributes to the transaction platform provided by the community, where the ultimate consensus-based bilateral trading prices have coordinated the operation of MGs.

WANG *et al.*: A HYBRID AGENT-BASED MODEL PREDICTIVE CONTROL SCHEME FOR SMART COMMUNITY ENERGY ...

579

TABLE I
PERFORMANCE COMPARISON BETWEEN PROPOSED DISTRIBUTED SCHEME, CENTRALIZED MPC SCHEME AND NONE-COOPERATING SCHEME

Scheme	Agent	Purchased energy (kWh)	Sold energy (kWh)	Trading fee ($)		Operation fee ($)	FR revenue ($)	Total revenue ($)	Mismatched energy (kWh)
				With MG	With main grid				
Proposed distributed MPC	CA	4141.9	11478.5	806.9	513.5		1325.4	1032.0	
	MG1	3335.3	937.4	114.9		139.8		−254.73	
	MG2	843.3	4788.3	−352.9		152.7		200.20	295.14
	MG3	641.7	3749.2	−278.9		281.3		−2.41	
	MG4	1322.0	2755.5	−153.7		234.7		−81.02	
	MG5	1041.1	2333.3	−136.3		257.9		−121.60	
Centralized MPC	CA	4139.7	11465.3	512.7	−512.7		1325.4	1325.40	
	MG1	2541.1	899.1	114.9		190.4		−305.33	
	MG2	637.7	4332.8	−258.6		129.5		129.19	97.05
	MG3	545.7	3168.9	−183.6		239.8		−56.21	
	MG4	975.6	2400.9	−99.7		230.5		−130.74	
	MG5	650.5	1873.8	−85.6		246.2		−160.54	
Non-cooperating MPC	MG1	3403.5	888.0	133.1		128.8		−262.00	
	MG2	832.8	4581.8	−316.5		132.9		183.60	
	MG3	601.0	3566.8	−249.2		264.6		−15.30	
	MG4	1337.9	2693.4	−135.2		226.7		−91.50	
	MG5	1031.1	2248.8	−118.0		248.6		−130.60	

2) Analysis on Transaction Results

Figure 2 illustrates the power transaction between CA and each MG and Fig. 3 demonstrates the corresponding control sequence of each MG. The lower bound of the buying price and the upper bound of the selling prices between CA and MGs are 40 $/MWh and 100 $/MWh, respectively, which can guarantee the profits of CA. The positive transactive power represents that the MG imports power from CA to MGs while the negative power means the MGs export power to CA. It can be found out that all MGs have done the transaction at the same prices thanks to the consensus-based interaction process.
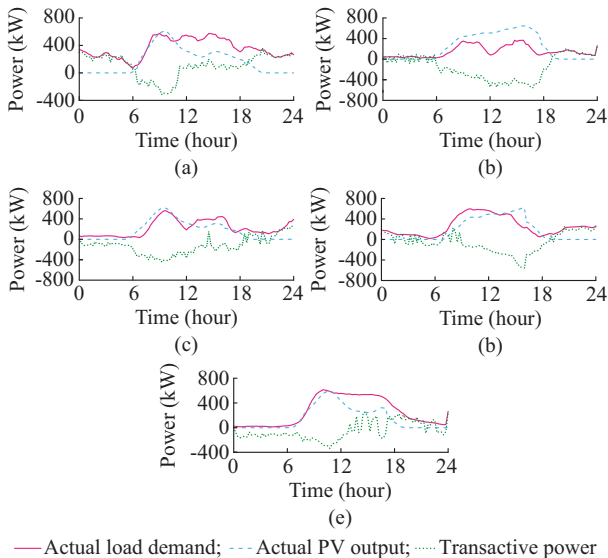

Fig. 3. Control sequences of MGs. (a) MG1. (b) MG2. (c) MG3. (d) MG4. (e) MG5.

P_{batt}; P_{DG}; P_{DR}; c_{buy}; c_{sell}

Actual load demand; Actual PV output; Transactive power

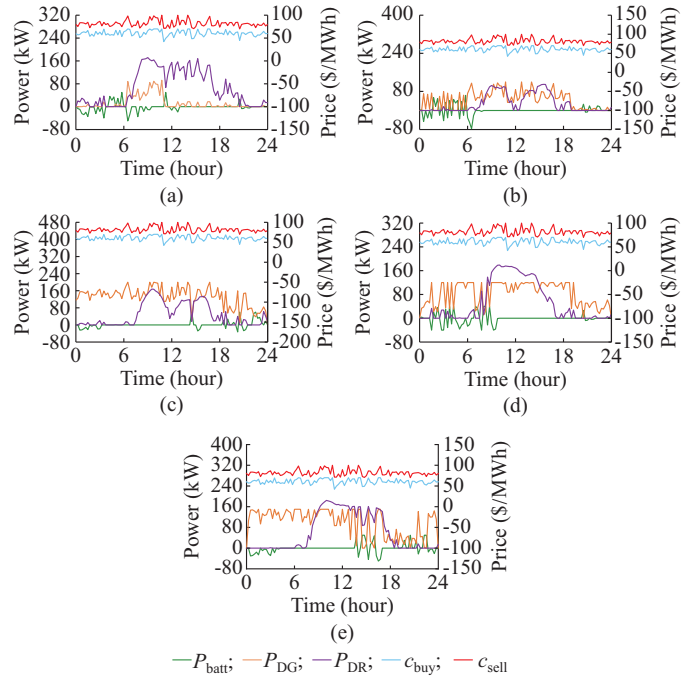Fig. 2. Power transaction between CA and MGs. (a) MG1. (b) MG2. (c) MG3. (d) MG4. (e) MG5.

Since each MG operates according to its local objective and intends to minimize its local cost, it can be observed that each of them tends to sell power when its PV generation is high, e.g., from hour 6 to hour 18 in MG2 and from hour 8 to hour 22 in MG4. And buying power as PV generation is not efficient to achieve the supply-demand balance in MG, e.g., from hour 0 to hour 6 in MG1 and from hour 18 to hour 24 in MG4. Though each MG is set with differential com-

ponent capacities and cost functions, the exported/imported power of the dispatchable devices is largely influenced by the consensus-based trading prices induced by multi-agent interaction. Taking MG1 as an example, from hour 0 to hour 6 and from hour 18 to hour 24, MG1 intends to purchase electricity from CA due to its insufficient supply status. However, the consensus-based trading prices are all relatively low, leading to little power generation of DG and nearly no implementation of the load curtailment. In addition, during this period, BESS has the potential to charge instead of discharge due to the optimistic expectation for future trading prices. An interesting phenomenon can be found here that BESS would intend to be charged from the controllable energy resources (i.e., DG and DR) to fulfill the future economic object owing to the MPC operation strategy, e.g., from hour 0 to hour 6 in MG1. And then, from hour 6 to hour 18, the increased buying and selling prices offered to MG1 have motivated MG1 to generate more power or curtail more load according to its own cost function. Note that MG1 would intend to utilize its own flexible energy devices to export more power to CA with the favorable transaction price during hour 6 to hour 12.

3) Impacts of Communication Interaction Topology

More representative case studies are presented to analyze the performance of the consensus-based strategy under different communication topologies. Two types of interaction topologies of the five-MG communities have been utilized to test the proposed scheme: ① star connection shown in Fig. 4(a); ② random connection in Fig. 4(b), which is also the topology setting in the previous simulation case.
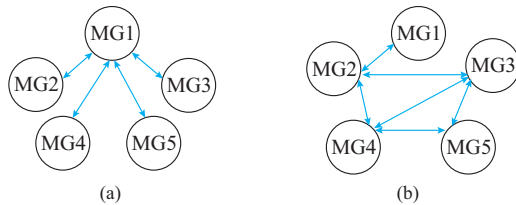
Fig. 4. Communication topologies of investigated MG community. (a) Star connection. (b) Random connection.

Figures 5 to 7 illustrate the evolution process of trading prices, tie-line power/mismatched power, and benefits of all MGs during the iterations under star connection and random connection at hour 16, respectively. It can be found that in one iteration cycle, all MGs are able to converge to the optimal trading price asymptotically and track the desired trajectories accurately irrespective of communication topologies. In addition, the ultimate results of consensus-based trading prices and iteration times are slightly different under these two communication topologies.

As shown in Fig. 5, the agreed selling price 72.47 $/MWh under the star connection is lower than 77.03 $/MWh under the random connection. By contrast, the agreed buying price 55.56 $/MWh under the star connection is higher than 51.22 $/MWh under the random connection. Thus, MGs interacting with adjacent MG agents in the star connection would bring more benefits to CA compared with the random connection. It is interesting to observe from Fig. 6 that all communication topologies (star connection or ran-

dom connection) can promote MGs to reach the ultimate consensus prices with little tracking deviation tolerance. Moreover, as illustrated in Fig. 7, the transaction cost of five MGs increases while the operation cost decreases with the consensus-based iterations. This is due to the declined tendency of selling and buying prices. As a result, MGs tend to buy power from CA instead of utilizing their own devices to generate power.
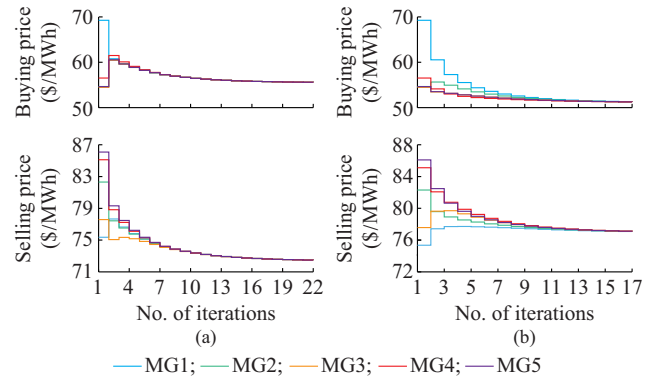
Fig. 5. Evolution process of trading prices among MGs under different communication topologies. (a) Star connection. (b) Random connection.
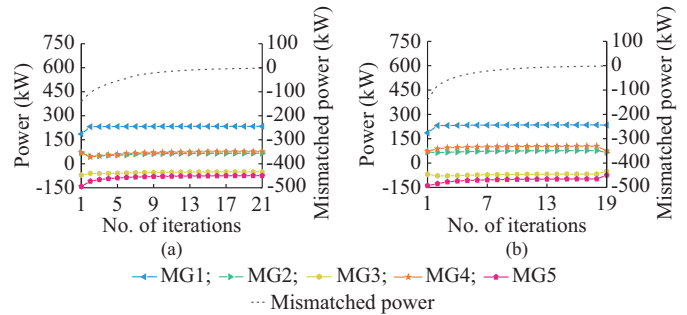
Fig. 6. Evolution process of tie-line power and mismatched power under different communication topologies. (a) Star connection. (b) Random connection.
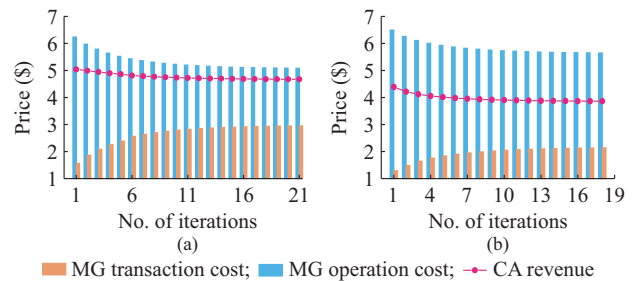
Fig. 7. Evolution process of the benefits of all agents under different communication topologies. (a) Star connection. (b) Random connection.

In addition, the topology of the communication network would also affect the convergence rate. The optimal results can be obtained in 21 iterations to reach an equilibrium point under star connection, while it only takes 19 iterations under the random connection.

4) Impacts of Adjustment Factor

The adjustment parameter is a key factor influencing the convergence speed. More case studies have been carried out to analyze the impact of parameter μ while other parameters

remain unchanged at the hour 17 (under random connection). Four cases with different adjustment parameter μ values have been tested: ① case A with $\mu = 4$; ② case B with $\mu = 10$; ③ case C with μ equaling to 20; ④ case D with $\mu = 25$. Figure 8 shows the evolution process of trading prices among agents in the four cases, while Fig. 9 further demonstrates all MGs can reach a final consensus with little tracking deviation, irrespective of different adjustment factors.
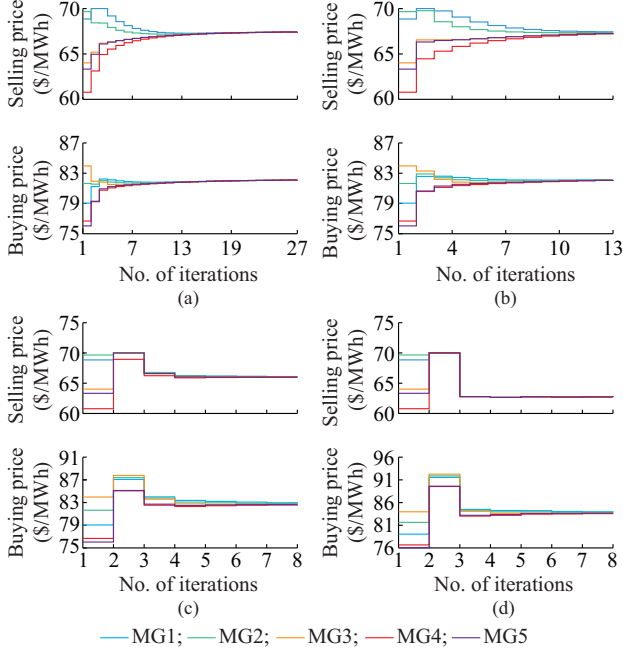

Fig. 8.   Evolution process of trading prices among MGs with different adjustment factors. (a) Case A. (b) Case B. (c) Case C. (d) Case D.
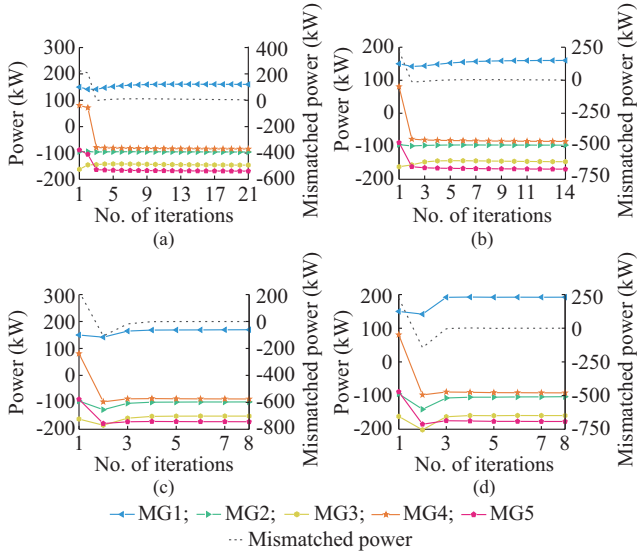

Fig. 9.   Evolution process of tie-line power and mismatched power with different adjustment factors. (a) Case A. (b) Case B. (c) Case C. (d) Case D.

As shown in Fig. 8, the consensus-based buying and selling prices are 67.43 $/MWh and 82.11 $/MWh in case A, respectively, while those for case B are nearly the same as case A. The agreed buying price 66.04 $/MWh in case C is lower while the agreed selling price 82.65 $/MWh is higher

compared with the prices of cases A and B. Furthermore, the buying and selling prices are 62.71 $/MWh and 83.65 $/MWh in case D, respectively, significantly different from the consensus prices in the previous cases. However, it is noticeable that the convergence speed has improved greatly with the increasing value of parameter μ. The simulation result illustrates that it takes 27 iterations to reach a consensus on the ultimate trading prices/quantity ($\mu = 4$), while the number of iterations decreases to 8 as the value of parameter μ increases to 20. The convergence rate does not elevate anymore as value μ exceeds a threshold. In fact, a very large μ may lead to instability, since the termination of iterations requires the amount of mismatched energy decreases to a certain value.

5) Impacts of Communication Failure

For practical applications, the imperfect communication network may cause the contact loss of some MGs during the interaction process at the lower level. To investigate that, more cases are conducted to test the robustness of the proposed scheme against the communication failure: ① case E: MG1 agent loses the contact with other MGs at the 10th iteration; ② case F: based on case E, MG1 agent reconnects with other MGs at the 30th iteration. Other parameters remain unchanged at the hour 15 (under random connection).

Figure 10 illustrates the evolution process of the trading prices for each MG in the case E and case F, while the iteration processes of the mismatched power and tie-line power of each agent are provided in Fig. 11.
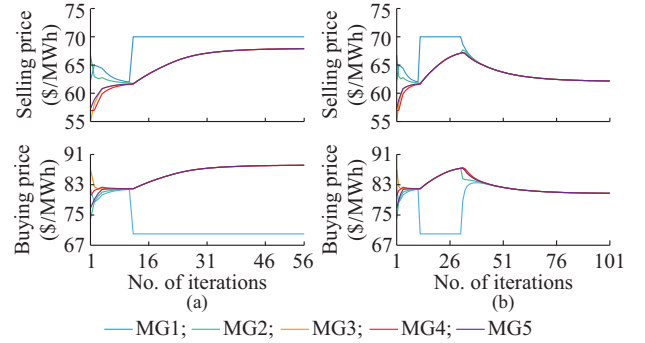

Fig. 10.   Evolution process of trading prices among MGs with communication failure. (a) Case E. (b) Case F.
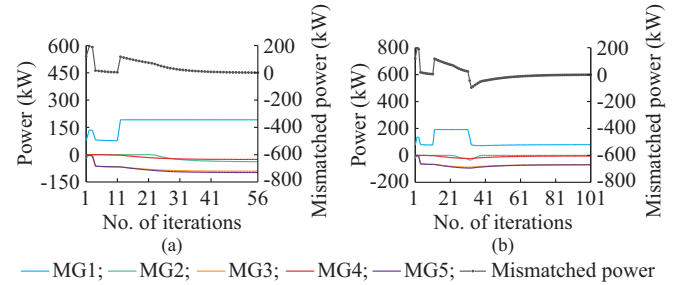

Fig. 11.   Evolution process of tie-line power and mismatched power with communication failure. (a) Case E. (b) Case F.

Note that once the MG1 agent is disconnected from the communication network, it will trade with CA at the price of grid rate (i.e., both the buying and selling prices are 70 $/

MWh) as shown in Fig. 10(a) and (b), which will highly affect its individual control process and lead to more mismatched power in the community, as shown in Fig. 11(a) and (b). Thanks to the on-going interaction process of other MGs, the disturbance brought by MG1 can be well handled, though it will take more iterations to reach convergence. Once the MG1 is reconnected to the communication network, the interaction process stays in the same manner as the previous cases, where the ultimate consensus-based transaction prices of all MGs reach nearly the same value. The simulation results have demonstrated the robustness of the proposed scheme against the communication failure.

6) Impacts of Uncertainties

Different degrees of uncertainties have been set to test the influences of the uncertain renewable energy and load demand on the proposed scheme. The reference energy trajectory of CA is presented as level A, while the predicted deviation $\Delta P_{L,m}^{\max}(k)$ and $\Delta P_{PV,m}^{\max}(k)$ have been set to be 0%, 5%, 10%, 15% of the prediction value, which are denoted as levels B, C, D, E, respectively. Figure 12 illustrates the power curves of tie-line between the CA and the main grid obtained by the proposed scheme under different uncertainty degrees on the day. It can be observed that the energy transaction between CA and the main grid is able to successfully track trajectory with negligible errors in the presence of uncertainties. The main reason is that the proposed energy management scheme is designed in an MPC framework, where these uncertainties have been effectively taken into account when implementing the controls. There may be another reason, that is, thanks to the consensus-based iteration process, the flexible bilateral transaction prices can be achieved to regulate the energy output/demand of all MGs.
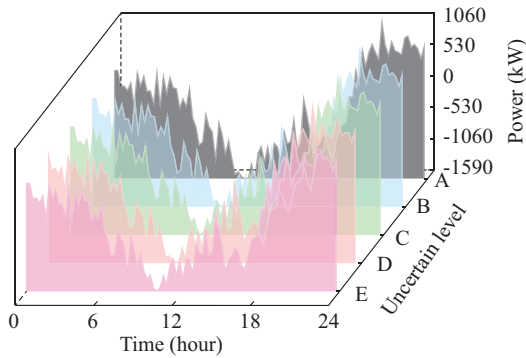

Fig. 12.   Tie-line power curves between CA and main grid under different levels of uncertainties.

IV. CONCLUSION

In this paper, a novel consensus-based distributed MPC scheme of multiple MGs within a smart community is proposed in the presence of uncertain renewable energy and load demand. The concept of community-based market together with the FR market provides an alternative choice for energy stakeholders in the community to gain economic improvement. A feasible interactive structure of the proposed scheme offers the transaction and information exchange platform, showing its great advantages on the coordination of multiple MGs and CA in a distributed manner. In particular,

the global target of CA can be successfully achieved with respect for interest and privacy of local MGs with efficient pricing rules. Numerical results have verified that the proposed scheme facilitates the participation of all agents, yielding a win-win situation. Meanwhile, thanks to the robustness of the proposed scheme, the uncertainties of PV power and load have been effectively taken into account. Future works involve incorporating peer-to-peer energy sharing market mechanism in a community. The possible malfunction of the communication system will be further investigated.

APPENDIX A

Due to the quadratic characteristics of the MG function, the transaction price c_m can be expressed as the linear function relating to $P_{tie,m}$, which is shown in (A1).

$$c_m = \alpha_m P_{tie,m} + \beta_m \tag{A1}$$

where α_m and β_m are the coefficients of MGm.

The pricing rules for MG coordination are represented in (24) and (25) at each iteration τ, which can be expressed as:

$$c_m^{\tau+1} = \sum_{n=1}^{M} d_{mn}^{\tau} c_m^{\tau+1} + \mu \Delta P^{\tau} \tag{A2}$$

$$P_{tie,m}^{\tau+1} = \frac{c_m^{\tau+1}}{\alpha_m} - \frac{\beta_m}{\alpha_m} \tag{A3}$$

$$\Delta P^{\tau+1} = \sum_{n=1}^{M} d_{mn}^{\tau} [\Delta P^{\tau} + (P_{tie,m}^{\tau+1} - P_{tie,m}^{\tau})] \tag{A4}$$

To analyze the convergence of the proposed consensus algorithm, the overall updating rules of (A1) to (A4) can be rewritten in the following matrix forms.

$$\boldsymbol{C}^{\tau+1} = \boldsymbol{D}\boldsymbol{C}^{\tau+1} + \mu\Delta\boldsymbol{P}^{\tau} \tag{A5}$$

$$\boldsymbol{P}^{\tau} = \boldsymbol{H}\boldsymbol{C}^{\tau+1} + \boldsymbol{F} \tag{A6}$$

$$\Delta\boldsymbol{P}^{\tau+1} = \boldsymbol{D}\Delta\boldsymbol{P}^{\tau} + \boldsymbol{D}(\boldsymbol{P}^{\tau+1} - \boldsymbol{P}^{\tau}) \tag{A7}$$

where $\boldsymbol{C}$, $\boldsymbol{P}$, $\Delta\boldsymbol{P}$ and $\boldsymbol{F}$ are the column vectors of c_m, $P_{tie,m}$, ΔP and $-\beta_m/\alpha_m$, respectively; and $\boldsymbol{H} = \mathrm{diag}(1/\alpha_1, 1/\alpha_2, ..., 1/\alpha_m)$. Define $[\boldsymbol{C}, \Delta\boldsymbol{P}]^{\mathrm{T}}$ as a new variable vector, the matrix can be expressed as:

$$\begin{bmatrix} \boldsymbol{C}^{\tau+1} \\ \Delta\boldsymbol{P}^{\tau+1} \end{bmatrix} = \begin{bmatrix} \boldsymbol{D} & \mu\boldsymbol{I}_m \\ \boldsymbol{DH}(\boldsymbol{D}-\boldsymbol{I}_m) & \boldsymbol{D}+\mu\boldsymbol{DH} \end{bmatrix} \begin{bmatrix} \boldsymbol{C}^{\tau} \\ \Delta\boldsymbol{P}^{\tau} \end{bmatrix} \tag{A8}$$

where $\boldsymbol{I}_m$ is an m-dimension identity matrix. Here, $\boldsymbol{G}$ is defined as:

$$\boldsymbol{G} = \begin{bmatrix} \boldsymbol{D} & \mu\boldsymbol{I}_m \\ \boldsymbol{DH}(\boldsymbol{D}-\boldsymbol{I}_m) & \boldsymbol{D}+\mu\boldsymbol{DH} \end{bmatrix} \tag{A9}$$

Equation (A10) demonstrates that if μ is small enough, the eigenvalue of G will be the same as D.

$$\left| \lambda\boldsymbol{I}_{2m} - \boldsymbol{G} \right| = \left| \lambda\boldsymbol{I}_m - \boldsymbol{D} \right|^2 + \mu \left| \boldsymbol{DH} \right| \left| \lambda\boldsymbol{I}_m - \boldsymbol{I}_m \right| \approx \left| \lambda\boldsymbol{I}_m - \boldsymbol{D} \right|^2 \tag{A10}$$

Moreover, $\boldsymbol{D}$ is a double-stochastic matrix with d_{nm} set in (24) in the model, where $\boldsymbol{D}\cdot\boldsymbol{1}_m = \boldsymbol{1}_m$. Since G and D share the same eigenvalue, the formulation of (A11) can be obtained.

$$\begin{bmatrix} \boldsymbol{D} & \mu\boldsymbol{I}_m \\ \boldsymbol{DH}(\boldsymbol{D}-\boldsymbol{I}_m) & \boldsymbol{D}+\mu\boldsymbol{DH} \end{bmatrix} \begin{bmatrix} \boldsymbol{1}_m \\ \boldsymbol{0}_m \end{bmatrix} = \begin{bmatrix} \boldsymbol{1}_m \\ \boldsymbol{0}_m \end{bmatrix} \tag{A11}$$

According to this proof, the system can converge to span $[\mathbf{1}_m, \mathbf{0}_m]^T$ as τ goes to infinity with small μ. Thus, c_m^τ is able to converge to a common value c_m^*, and the value of ΔP_m gradually decreases.

APPENDIX B

TABLE BI
PARAMETERS OF MGS

Agent	$P_{\text{DG},m}^{\max}$ (kW)	$E_{\text{BESS},m}^{\max}$ (kWh)	$E_{\text{BESS},m}^{\min}$ (kWh)	$P_{\text{ch},m}^{\max}/P_{\text{dis},m}^{\max}$ (kW)	$P_{\text{buy},m}^{\max}/P_{\text{sell},m}^{\max}$ (kW)	$\eta_{\text{ch}}/\eta_{\text{dis}}$
MG1	150	200	20	100	500	0.9
MG2	140	500	50	50	500	0.9
MG3	200	400	40	125	500	0.9
MG4	120	300	30	80	500	0.9
MG5	150	200	20	50	500	0.9

TABLE BII
OPERATING COST COEFFICIENTS OF DGS AND DR PROGRAM OF MGS

Agent	Operation cost coefficient of DG			Operation cost coefficient of DR		Operation cost coefficients of BESS α_{BESS}
	α_{DG}	β_{DG}	γ_{DG}	α_{DR}	β_{DR}	
MG1	1.52	63	200	−0.009	0.8	8000
MG2	1.02	60	167	−0.009	0.8	9000
MG3	0.76	42	133	−0.009	0.8	10000
MG4	1.78	48	133	−0.009	0.8	9000
MG5	1.27	54	100	−0.009	0.8	8000

REFERENCES

[1] J. Zeng, Q. Wang, J. Liu et al., "A potential game approach to distributed operational optimization for microgrid energy management with renewable energy and demand response," IEEE Transactions on Industrial Electronics, vol. 66, no. 6, pp. 4479-4489, Jun. 2019.

[2] Y. Liu, K. Zuo, J. Liu et al., "Dynamic pricing for decentralized energy trading in micro-grids," Applied Energy, vol. 288, no. 1, pp. 689-699, Oct. 2018.

[3] C. Essayeh, M. R. Fenni, and H. Dahmouni, "Optimization of energy exchange in microgrid networks: a coalition formation approach," Protection and Control of Modern Power System, vol. 4, no. 24, pp. 1-10, Dec. 2019.

[4] W. Liu, J. Zhan, and C. Y. Chung, "A novel transactive energy control mechanism for collaborative networked microgrids," IEEE Transaction on Power Systems, vol. 34, no. 3, pp. 2048-2060, May 2019.

[5] T. Sousa, T. Soares, P. Pinson et al., "Peer-to-peer and community-based markets: a comprehensive review," Renewable and Sustainable Energy Reviews, vol. 104, pp. 367-378, Apr. 2019.

[6] F. Moret and P. Pinson, "Energy collectives: a community and fairness based approach to future electricity markets," IEEE Transactions on Power Systems, vol. 34, no. 5, pp. 3994-4004, Sept. 2019.

[7] C. Wouters, E. S. Fraga, and A. M. James, "An energy integrated, multi-microgrid, MILP (mixed-integer linear programming) approach for residential distributed energy system planning: a South Australian case-study," Energy, vol. 85, pp. 30-44, Jun. 2015.

[8] S. D. Beigvand, H. Abdi, and M. L. Scala, "Hybrid gravitational search algorithm-particle swarm optimization with time varying acceleration coefficients for large scale CHPED problem," Energy, vol. 126, pp. 841-853, May 2017.

[9] S. M. Amin, "Smart grid security, privacy, and resilient architectures: opportunities and challenges," in Proceedings of 2012 IEEE PES General Meeting, San Diego, USA, Jul. 2012, pp. 1-2.

[10] R. Kumar, M. J. Wenzel, M. J. Ellis et al., "A stochastic model predictive control framework for stationary battery systems," IEEE Transactions on Power Systems, vol. 33, no. 4, pp. 4397-4406, Jul. 2018.

[11] B. P. Koirala, E. Koliou, J. Friege et al., "Energetic communities for community energy: a review of key issues and trends shaping integrated community energy systems," Renewable and Sustainable Energy Reviews, vol. 56, pp. 722-744, Apr. 2016.

[12] Z. Zhang and M. Chow, "Convergence analysis of the incremental cost consensus algorithm under different communication network topologies in a smart grid," IEEE Transactions on Power Systems, vol. 27, no. 4, pp. 1761-1768, Nov. 2012.

[13] Z. Tang, D. J. Hill, and T. Liu, "A novel consensus-based economic dispatch for microgrids," IEEE Transactions on Smart Grid, vol. 9, no. 4, pp. 3920-3922, Jul. 2018.

[14] V. P. Singh, N. Kishor, and P. Samuel, "Distributed multi-agent system-based load frequency control for multi-area power system in smart grid," IEEE Transactions on Industrial Electronics, vol. 64, no. 6, pp. 5151-5160, Jun. 2017.

[15] T. Morstyn and M. D. McCulloch, "Multiclass energy management for peer-to-peer energy trading driven by prosumer preferences," IEEE Transactions on Power Systems, vol. 34, no. 5, pp. 4005-4014, Sept. 2019.

[16] W. Tushar, B. Chai, C. Yuen et al., "Energy storage sharing in smart grid: a modified auction-based approach," IEEE Transactions on Smart Grid, vol. 7, no. 3, pp. 1462-1475, May 2016.

[17] P. Tian, X. Xiao, K. Wang et al., "A hierarchical energy management system based on hierarchical optimization for microgrid community economic operation," IEEE Transactions on Smart Grid, vol. 7, no. 5, pp. 2230-2241, Sept. 2016.

[18] F. Garcia-Torres, C. Bordons, and M. A. Ridao, "Optimal economic schedule for a network of microgrids with hybrid energy storage system using distributed model predictive control," IEEE Transactions on Industrial Electronics, vol. 66, no. 3, pp. 1919-1929, Mar. 2019.

[19] M. Fathi and H. Bevrani, "Statistical cooperative power dispatching in interconnected microgrids," IEEE Transactions on Sustainable Energy, vol. 4, no. 3, pp. 586-593, Jul. 2013.

[20] D. Gregoratti and J. Matamoros, "Distributed energy trading: the multiple-microgrid case," IEEE Transactions on Industrial Electronics, vol. 62, no. 4, pp. 2551-2559, Apr. 2015.

[21] H. Qiu, B. Zhao, W. Gu et al., "Bi-level two-stage robust optimal scheduling for AC/DC hybrid multi-microgrids," IEEE Transactions on Smart Grid, vol. 9, no. 5, pp. 5455-5466, Sept. 2018.

[22] H. Wang and J. Huang, "Incentivizing energy trading for interconnected microgrids," IEEE Transactions on Smart Grid, vol. 9, no. 4, pp. 2647-2657, Jul. 2018.

[23] K. Dehghanpour and H. Nehrir, "Real-time multiobjective microgrid power management using distributed optimization in an agent-based bargaining framework," IEEE Transactions on Smart Grid, vol. 9, no. 6, pp. 6318-6327, Nov. 2018.

[24] G. E. Rahi, S. R. Etesami, W. Saad et al., "Managing price uncertainty in prosumer-centric energy trading: a prospect-theoretic stackelberg game approach," IEEE Transactions on Smart Grid, vol. 10, no. 1, pp. 702-713, Jan. 2019.

[25] H. Li, A. T. Eseye, J. Zhang et al., "Optimal energy management for industrial microgrids with high-penetration renewables," Protection and Control of Modern Power System, vol. 2, no. 12, p. 12, Apr. 2017.

[26] Y. Liu, H. B. Gooi, Y. Li et al., "A secure distributed transactive energy management scheme for multiple interconnected microgrids considering misbehaviors," IEEE Transactions on Smart Grid, vol. 10, no. 6, pp. 5975-5986, Nov. 2019.

[27] D. Wu, T. Yang, A. A. Stoorvogel et al., "Distributed optimal coordination for distributed energy resources in power systems," IEEE Transactions on Automation Science and Engineering, vol. 14, no. 2, pp. 414-424, Apr. 2017.

[28] X. Zhang, T. Yu, Z. Xu et al., "A cyber-physical-social system with parallel learning for distributed energy management of a microgrid," Energy, vol. 165, pp. 205-221, Dec. 2018.

[29] P. Kou, D. Liang, and L. Gao, "Distributed EMPC of multiple microgrids for coordinated stochastic energy management," Applied Energy, vol. 185, pp. 939-952, Jan. 2017.

Xiaodi Wang received the B.Sc. degree in electrical engineering from Sichuan University, Chengdu, China, in 2016, where she is currently working toward the Ph.D. degree at the College of Electrical Engineering, Sichuan University. Her current research interests include energy market design and distributed energy management.

Youbo Liu received the B.Sc., M.Sc., and Ph.D. degrees from Sichuan University, Chengdu, China, in 2005, 2008, and 2011, respectively. He is currently an Associate Professor in power system with the College of Electric Engineering, Sichuan University. His research interests mainly include ma-

chine learning in smart grid, energy storage system applications, etc.

Junbo Zhao received the Ph. D. degree from Virginia Tech, Falls Church, USA, in 2018. He is currently with the Department of Electrical and Computer Engineering, Mississippi State University, Starkville, USA. He has written two book chapters and published more than 40 peer-reviewed journal and conference papers. He serves as the Associate Editor of the International Journal of Electrical Power and Energy Systems and the IET Generation, Transmission and Distribution. He is currently the Chair of the IEEE Task Force on Power System Dynamic State and Parameter Estimation, the Secretary of the IEEE Working Group on State Estimation Algorithms, and the IEEE Task Force on Synchrophasor Applications in Power System Operation and Control. His research interests include power system real-time monitoring, operation and cyber security that include estimation, dynamics and stability, cyber-attacks and countermeasures, big-data analytics, and robust statistics with applications in the smart grid.

Junyong Liu received the Ph. D. degree from Brunel University, London, U.K., in 1998. He is currently a Professor with the College of Electric Engineering, Sichuan University, Chengdu, China. His main research interests include power system planning, operation, stability, and power market.